Article

Discovery Medicine 2025; 37(201): 2178–2191
https://doi.org/10.24976/Discov.Med.202537201.185

Targeting BTRC to Restore ULK1-Mediated Autophagy in Macrophages: A Novel Strategy Against Post-Traumatic Bacterial Pneumonia

Limei Tian[1,*], Lishan Zhang[1]

[1]Department of Pediatrics, Wucheng District People's Hospital, 321001 Jinhua, Zhejiang, China
*Correspondence: tianlimei222@163.com (Limei Tian)
Submitted: 4 July 2025 Revised: 12 September 2025 Accepted: 17 September 2025 Published: 20 October 2025

Background: Autophagy is essential for effective bacterial clearance, in which the E3 ubiquitin ligase beta-transducin repeat containing E3 ubiquitin protein ligase (BTRC) participates. Herein, investigation was performed regarding the role of BTRC in post-traumatic brain injury (TBI)-associated bacterial pneumonia, alongside elucidation of the downstream mechanisms involving Unc-51 like autophagy activating kinase 1 (ULK1).

Methods: Using post-TBI mouse models and primary alveolar macrophages (PAM), we examined the effects of *Pseudomonas aeruginosa* K-strain (PAK) infection and BTRC silencing on pulmonary inflammation and bacterial clearance. Inflammatory cytokines, lung pathology and PAM viability were analyzed. Bacterial clearance in lung tissues, as well as intracellular killing and phagocytosis in PAM, was evaluated by colony-forming assays. Expressions of autophagy-related markers were measured employing western blot and immunofluorescence. ULK1 ubiquitination was assessed via immunoprecipitation. To confirm the involvement of ULK1, experiments with both BTRC and ULK1 knockdown were performed.

Results: PAK infection impaired bacterial clearance, suppressed autophagy and increased inflammatory cytokine levels in both lung tissues and PAMs, while these pathological changes were significantly reversed by BTRC knockdown ($p < 0.01$). Mechanistically, PAK infection promoted ULK1 ubiquitination in PAMs, which was offset by BTRC silencing; however, ULK1 knockdown neutralized the effects of BTRC silencing, as indicated by repressed autophagy activity and bacterial clearance, and enhanced inflammatory responses ($p < 0.05$).

Conclusion: BTRC silencing alleviates PAK-induced bacterial pneumonia after TBI by enhancing macrophage-mediated bacterial clearance through inhibition of ULK1 ubiquitination and activation of autophagy, a process critically dependent on ULK1 stability.

Keywords: beta-transducin repeat containing E3 ubiquitin protein ligase; unc-51 like autophagy activating kinase 1; ubiquitination; autophagy; traumatic brain injury; bacterial pneumonia

Introduction

Traumatic brain injury (TBI) is recognized as brain tissue damage caused by traumatic factors, with high morbidity and disability rates [1,2]. The current treatment of TBI focuses on the prevention of secondary brain injury, which is crucial to the prognosis. As previously proved, lung infection, as a common complication after TBI, has high incidence [1–5]. Therefore, relieving post-TBI lung infection contributes to improving the prognosis of the TBI.

Bacterial pneumonia is the most common type of pneumonia, primarily resulting from *Haemophilus influenzae*, *Staphylococcus aureus*, *Pseudomonas aeruginosa*, etc. *Pseudomonas aeruginosa* is a predominant pathogen responsible for lung infection following TBI [1,6]. More importantly, a previous study indicated that the decreased bacterial clearance is associated with a higher mortality in the post-TBI mouse models [1]. Thus, the current study concentrates on bacterial clearance after TBI. Reportedly, macrophages and neutrophils are involved in bacterial clearance of lung infection [7], with neutrophils exerting a bactericidal effect [8]. Autophagy also plays an irreplaceable role in actively promoting bacterial clearance [9], particularly in *Pseudomonas aeruginosa*-induced lung infection [7]. Interestingly, autophagosome formation can lead to enhanced bacterial clearance [7]. Unc-51 like autophagy activating kinase 1 (ULK1) boosts PIKfyve-containing autophagosome formation, thereby enhancing the autophagy [10]. Accordingly, we have reason to believe that ULK1 plays an active role in the bacterial clearance after TBI via facilitating autophagy. However, the role of ULK1 in TBI has been poorly defined.

Furthermore, we investigated ubiquitination, one of the most prevalent post-translational modifications in the proteome, and widely participating in various physiological processes, including transcriptional regulation, DNA

damage repair, cell cycle, apoptosis, etc. [11]. Based on the existing research, as a E3 ligase, beta-transducin repeat containing E3 ubiquitin protein ligase (BTRC) can target various key regulators for degradation and ubiquitination to greatly impair the tumorigenesis, autophagy, cell cycle progression, etc. [12]. Recent findings revealed that BTRC can degrade ULK1 by ubiquitination [13]. More interestingly, inhibition of autophagy attenuates the bactericidal effect of alveolar macrophages, which is accompanied by a lower expression of ULK1 [14]. Moreover, lipopolysaccharides (LPS)-stimulated BTRC can interact with protein kinase D1 (PKD1) and promote PKD1 downregulation, which in turn restricts TNF receptor-associated factor 6 (TRAF6)-I kappa B kinase (IKK) signaling upstream of IkBα in LPS inflammatory pathway [15]. Nevertheless, there is a knowledge gap when it comes to the corresponding mechanism of BTRC silencing in lung infection after TBI, which has thus become one of the objectives in our research. Given all that, we have hypothesized that BTRC silencing can effectively regulate the bacterial clearance after TBI via regulating ULK1 ubiquitination and autophagy.

In the current study, we explored whether BTRC silencing can improve bacterial pneumonia after TBI by enhancing the bacterial clearance of macrophages via ULK1 ubiquitination and autophagy, which may provide a promising therapeutic avenue.

Materials and Methods

Post-TBI Pneumonia Models and Transfection

48 male C57BL/6 mice (20–25 g) were obtained from Hangzhou Medical College (China) and housed under 12/12 h light/dark cycles (40–70% humidity, 37 °C).

Post-TBI pneumonia animal modeling referred to previous studies [1,16]. In brief, the mice were maintained in a stereotaxic frame (BLAB-ST-8001, David Kopf Instrument, Tujunga, CA, USA) with head holder and ear bars, and then anesthetized with 0.3% pentobarbital sodium (50 mg/kg, P3761, Haoran Biological Technology, Shanghai, China). Later, the top of the skull was incised (1 cm) to expose the bone. An electrical drill (Model 1474, David Kopf Instrument, Tujunga, CA, USA) that was fixed on the stereotaxic arm was applied to carry out a 5 mm craniotomy on the right parietotemporal cortex. After that, an electromagnetic impact device (Benchmark™ Stereotaxic Impactor, Leica Biosystems, Buffalo Grove, IL, USA) was used to induce a controlled cortical impact injury in mice, during which tissue displacement, the speed, and the impact duration were 1 mm, 5 m/second (s), and 400 ms. Then, the skin of the mice was sutured and the mice were put on warming cushions for approximately 1 to 2 h. When the mice were able to move freely, they were housed in the cages again. 24 h later, the mice were evaluated for behavioral testing. Modified neurologic severity scoring (mNSS) was performed based on the study of Li *et al.* [17]. 24 h after the surgery, the mice in the TBI group showed a substantial increase in mNSS (>6), indicating successful modeling. One mouse in the Mod group died during the surgery. Then the anesthetized mice underwent craniotomy, and 25 µL phosphate buffer saline (PBS, 806552, Merck Millipore, Boston, MA, USA) with colony-forming units of *Pseudomonas aeruginosa* K-strain (PAK, 53308, American Type Culture Collection, Manassas, VA, USA) was instilled to the lungs of the mice through the tracheae, followed by 15-min recovery for the mice. Finally, the mice were housed in the cages.

Transfection of siRNA was performed 24 h after PAK infection in the post-TBI pneumonia model with reference to a previous study [18]. Prior to the transfection, the siRNAs targeting BTRC (siBTRC, forward (F): 5′-ACUGUUUCUUGGUUUAAGCAG-3′; reverse (R): 5′-GCUUAAACCAAGAAACAGUAU-3′) and ULK1 (siULK1, F: 5′-GAGCAAGAGCACACGGAAA-3′; R: 5′-UUUCCGUGUGCUCUUGCUC-3′), along with corresponding negative control siRNAs (small interfering RNA targeting negative control (siNC) for BTRC, F: 5′-UAAGGCUAGCAAUAAUCGCUUTT-3′; R: 5′-AAGCGAUUAUUGCUAGCCUUAGTT-3′; siNC for ULK1, F: 5′-UCAAGACUUCUGGUAAUUCUGTT-3′; R: 5′-CAGAATTACCAGAAGUCUUGATT-3′), were synthesized by GenePharma (Shanghai, China). The mice were intravenously treated with 100 µL siBTRC or/and siULK1 (1 mg/kg) packaged into hydration of a freeze-dried matrix lipid nanoparticles by retro-orbital administration [19].

Finally, all mice used were anesthetized with sodium pentobarbital (50 mg/kg, P3761, Sigma-Aldrich, St. Louis, MO, USA) and sacrificed by cervical dislocation 36 h after PAK infection. Later, the lung tissues were harvested for following experiments, and the thoracic cavity and trachea were collected to obtain bronchoalveolar lavage (BAL) fluid. 1-mL syringe with an angiocath was applied to make an incision in the trachea, and lung lavage was carried out using 1 mL PBS supplemented with 1% fetal bovine serum (FBS) thrice, thereby gaining the BAL fluid.

Grouping

For subsequent analyses, four groups of mice were established (n = 6/group): Sham group (PAK injection); Mod group (craniotomy and PAK injection); Mod+siNC group (craniotomy, PAK injection, and siNC transfection); Mod+siBTRC group (craniotomy, PAK injection, and siBTRC transfection).

Mice were randomly assigned into four groups (n = 6/group): Sham group (PAK injection); Mod+siNC+siNC (craniotomy, PAK injection, and siNC for ULK1 and siNC for BTRC transfection); Mod+siBTRC+siNC (craniotomy, PAK injection, and siNC for ULK1 and siBTRC transfection); Mod+siBTRC+siULK1 (craniotomy, PAK injection, and siULK1 and siBTRC transfection).

Enzyme-Linked Immunosorbent Assay (ELISA)

Tumor necrosis factor α (TNF-α), interleukin 1β (IL-1β), interleukin 6 (IL-6), and interferon-γ (IFN-γ) in BAL fluid were detected by ELISA kits of TNF-α (CSB-E04741m(1), sensitivity: 15.6 pg/mL, detection range: 62.5–4000 pg/mL, Cusabio, Houston, TX, USA), IL-1β (88-7013-88, sensitivity: 8 pg/mL, detection range: 8–1000 pg/mL, Thermo Fisher Scientific, Waltham, MA, USA), IL-6 (KMC0061, sensitivity: <3 pg/mL, detection range: 0.32–5000 pg/mL, Thermo Fisher Scientific, Waltham, MA, USA), and IFN-γ (CSB-E04578m(1), sensitivity: 0.039 ng/mL, detection range: 0.156–10 ng/mL, Cusabio, Houston, TX, USA).

TNF-α and IFN-γ levels were measured according to the instructions. After post-TBI pneumonia modeling, BAL fluid was obtained and collected in 96-well plates, and cultured with 100 µL standard solution and medium (2 h, 37 °C). Afterwards, incubation with 100 µL Biotin-antibody (1:100) (1 h, 37 °C), 100 µL HRP-avidin (1 h, 37 °C), and 90 µL TMB Substrate (darkness, 15–30 min, 37 °C) was performed, which was later terminated employing 50 µL Stop solution. The optical density (OD) value (450 nm) was measured using Infinite M200 microplate reader (30190085, Tecan, Männedorf, Switzerland).

IL-1β and IL-6 levels in BAL fluid were assessed following the instructions. In short, 100 µL BAL fluid in each well of a 96-well plate underwent 2-h incubation. Later, 100 µL Ms IL-6 Biotin Conjugate solution (1:250) (30 min), 100 µL streptavidin-HRP solution (30 min), and 100 µL Stabilized Chromogen (30 min, darkness, room temperature (RT)) were separately added for incubation. Following the addition of 100 µL stop solution, the OD value (450 nm) was measured as aforementioned.

Taking the concentration of the standard substance as the abscissa and the OD value as the ordinate, a standard curve was drawn. Based on the OD value of the sample, the corresponding concentration was found from the standard curve and then multiplied by the dilution factor to obtain the actual concentration of each sample.

Hematoxylin and Eosin (HE) Staining

After the post-TBI pneumonia modeling and lung tissue collection, the lung tissues underwent fixation (10% formalin, G2160, Solarbio, Beijing, China) and embedment (paraffin, YA0012, Solarbio, Beijing, China) to obtain the tissue blocks. Then the blocks were cut into 4 µm thickness, dewaxed (xylene, 1330-20-7, Merck Millipore, Burlington, MA, USA), and rehydrated (ethanol gradient). Afterwards, the tissues were stained with Hematoxylin Staining Solution (C0107, Beyotime, Shanghai, China) (5 min) and Eosin Y solution (G1100, Solarbio, Beijing, China) (2 min), and rinsed by distilled water, followed by observation under a microscope (100× or 400× magnification; TS100, Nikon, Tokyo, Japan) [20].

Primary Alveolar Macrophages (PAM) Isolation

PAM obtainment followed a previous study [14]. The BAL fluid was collected from sacrificed model mice, centrifuged (1000 ×g, 10 min, 4 °C). With supernatant removal, resuspension in Dulbecco's Modified Eagle's Medium (DMEM, M012-500, VectorBuilder, Guangzhou, China) with 10% FBS and 1-h incubation (5% CO_2, 37 °C) for the attachment of macrophages were conducted. Finally, the normal saline was employed to clear the non-adherent cells. Cells have been tested for mycoplasma and were free of contamination.

PAM Identification

PAM were cultured in a petri dish with a sterile cover glass or cell climbing slide placed inside. After the cells adhered to the wall and grew to an appropriate density (about 70–80% confluence), staining was carried out. The climbing slide was completely covered with Crystal Violet Staining Solution (C0121-100ml, Beyotime, Shanghai, China) and colored for 10 min. The cell morphology was observed under an optical microscope (DP73, OLUMPUS, Tokyo, Japan).

2×10^5 cells were incubated (4 °C, 30 min) with PBS solution containing the manufacturer-recommended conjugated monoclonal antibodies (mAbs) for specific mouse antigens, namely fluorescein isothiocyanate (FITC)-conjugated rat anti-SiglecF (155503, BioLegend, San Diego, CA, USA), mouse anti-CD11c (11-0114-82), anti-CD64 (17-0641-82) or anti-CD11b (12-0112-85) (the latter two from Invitrogen, San Diego, CA, USA). Next, each cell population was washed twice with chilled FACS buffer (PBS containing 5% FBS). To remove dead cells in flow cytometry analysis, each final cell pellet was resuspended in FACS buffer containing 50 µg propidium iodide (Invitrogen, Carlsbad, CA, USA) before analysis. All samples were then evaluated using a CytoFLEX flow cytometer (Beckman Coulter, La Brea, CA, USA), and the result data were analyzed using FlowJo software (v.10.0.8, TreeStar, San Carlos, CA, USA).

Cell Transfection

Prior to the transfection, siBTRC (5′-CTGGACCACATCGGTGAGAA-3′), ULK1 (siULK1, F: 5′-GCACAGAGACCGUGGGCAA-3′), and siNC (5′-UUCUCUAACUCGAUACAGGAUTT-3′) were synthesized by GenePharma. Then Lipofectamine™ 3000 Transfection Reagent (L3000015, Thermo Fisher Scientific, Waltham, MA, USA) was used for the transfection of siBTRC/siNC into PAM. When cell confluence reached 90% in a 96-well plate, transfection was performed. Opti-MEM™ medium (31985062, Thermo Fisher Scientific, Waltham, MA, USA) was used for dilution of Lipofectamine™ 3000 reagent. SiRNA was diluted in Opti-MEM™ medium, and reacted with diluted Lipofec-

tamine™ 3000 reagent (10 min, RT). Next, siRNA-lipid complexes were added into PAM for transfection (48 h, 37 °C).

Cell Treatment

PAM were assigned to control (Con; DMEM incubation), model (Mod; DMEM incubation and 2-h PAK infection (a multiplicity of infection (MOI) of 20:1 bacteria-cell ratio)) [14], Mod+siNC, Mod+siBTRC, Mod+siNC+siNC, Mod+siBTRC+siNC, and Mod+siBTRC+siULK1 groups. For siRNA-related groups, PAM were first transfected (48 h) with siNC for BTRC, siBTRC, siNCs for ULK1 and BTRC, and siBTRC + siNC for ULK1, and siBTRC + siULK1. Later, the PAM were maintained in the DMEM, and infected by the PAK in an MOI of 20:1 bacteria-cell ratio for 2 h.

Cell Counting Kit 8 (CCK-8) Assay

PAM transfected with/without siBTRC and infected with PAK were subjected to cell viability measurement using CCK-8 kit (abs50003, Absin, Shanghai, China). In brief, 100 µL PAM (1×10^3 cells/well) were cultured in a 96-well plate (24 h), and reacted with 10 µL CCK-8 solution (4 h). Finally, the OD value (450 nm) was assessed by the microplate reader.

Colony Forming Unit (CFU) Count Assay

The bacterial clearance in lung tissues, and the intracellular killing and phagocytosis of PAM on PAK were evaluated through CFU count assay. As for the bacterial clearance, after the mice instilled with PAK were sacrificed, the lung tissues were obtained and homogenized. The homogenates were diluted continuously and placed on sheep-blood agar plates. The number of CFU was normalized to that of CFU at bacterial entry (30 min/time) [1,21].

As for the intracellular killing and phagocytosis of PAM on PAK, the PAM received PAK infection and 1-h incubation in the DMEM. To estimate the number of internalized PAK post 1-h incubation, following the indicated processing, 300 µg/ml gentamicin (YZ-130326, Solarbio, Beijing, China) was added into the DMEM (30 min) to disrupt the extracellular PAK, and the hemocytometer (Countess™ 3, Thermo Fisher Scientific, Waltham, MA, USA) was employed to count cells. Later, the cells were lysed, and the CFU of the PAK was measured. Finally, the internalized PAK was determined using the formula (CFU (1 h)/Cell number). To analyze the number of the viable PAK after 2-h incubation, 300 µg/mL gentamicin (YZ-130326, Solarbio, Beijing, China) was added to kill the extracellular PAK, and the PAM were incubated (1 h) and lysed to analyze the CFU of the intracellular PAK. Finally, the killing efficiency was determined using the formula [CFU (1 h)-CFU (2 h)]/CFU (1 h) [14].

Immunofluorescence Staining

After the PAM transfected with/without siBTRC were exposed to PAK, the microtubule-associated protein 1 light chain 3 (LC3) expression was assessed via immunofluorescence staining. In brief, the PAM were cultured in a 24-well plate (24 h), fixed with 4% paraformaldehyde (P1110, Solarbio, Beijing, Chian), and permeabilized using 0.2% Triton-X-100 (P0096, Beyotime, Shanghai, China). Afterwards, the cells were maintained in 5% BSA (SW3015, Solarbio, Beijing, China), and incubated with primary LC3 antibody (ab128025, 0.5 µg/mL, Abcam, Cambridge, UK) and Goat Anti-Rabbit IgG (Alexa Fluor® 488, ab150077, 1/1000, Abcam, Cambridge, UK), followed by cell nuclei staining in 4',6-diamidino-2-phenylindole (DAPI, C1002, Beyotime, Shanghai, China). Finally, cell observation was completed with IX71 microscope (200× magnification; Olympus, Tokyo, Japan).

Western Blot

BTRC, ULK1, LC3 I, LC3 II, and P62 expression levels in lung tissues and PAM transfected with/without siBTRC and infected by PAK were measured by western blot. Concretely, following total protein isolation from PAM and lung tissues using RIPA Lysis Buffer (E-BC-R327, Elabscience, Wuhan, China), protein concentration was tested with BCA protein quantification kit (ab102536, Abcam, Cambridge, UK). Later, the protein samples were electrophorized in 12% and 6% sodium dodecyl sulfate polyacrylamide gel electrophoresis (SDS-PAGE) gels (P0672, P0676, Beyotime, Shanghai, China), and were transferred onto PVDF membranes (abs932, Absin, Shanghai, China). Next, the membranes were blocked with 5% non-fat skim milk (D8340, Solarbio, Beijing, China) diluted in Tris Buffered Saline with Tween-20 (TBST, T1085, Solarbio, Beijing, China) (2 h, RT), and cultured (4 °C, overnight) with primary antibodies: BTRC (1 µg/mL, PA5-69160, 60 kDa, Invitrogen, Waltham, MA, USA), ULK1 (1 µg/mL, ab167139, 112 kDa, Abcam, Cambridge, UK), P62 (1:10,000, ab109012, 62 kDa, Abcam, UK), LC3 (1:2000, ab192890, 14/16 kDa, Abcam, Cambridge, UK), and GAPDH (1:1000, ab8245, 37 kDa, Abcam, Cambridge, UK). The horseradish peroxidase (HRP) labeled Rabbit anti-Mouse IgG (1:2000, ab6728, Abcam, Cambridge, UK) and Mouse anti-Rabbit IgG (1:1000, ab99697, Abcam, Cambridge, UK) were additionally incubated with the membrane (RT, 1 h). Finally, the band signals were analyzed by ECL reagent kits (FP300, ABP Biosciences, Rockville, MD, USA) on Tanon 5200 imaging system (Tanon, Shanghai, China), and quantitative analyses were performed using ImageJ software (1.52s version, National Institutes of Health, Bethesda, MD, USA).

Table 1. Sequences of the gene primers used in QRT-PCR

Gene	Forward (5′-3′)	Reverse (5′-3′)
BTRC	TGCCCAAGCAACGGAAACT	GCCCATGTTGGTAATGACACA
ULK1	AGCCACCCTTTTCCTACCAG	TTCTTGGAGAGTGCTCAGGC
GAPDH	AGGTCGGTGTGAACGGATTTG	TGTAGACCATGTAGTTGAGGTCA

BTRC, beta-transducin repeat containing E3 ubiquitin protein ligase; *ULK1*, Unc-51 like autophagy activating kinase 1; *GAPDH*, glyceraldehyde-3-phosphate dehydrogenase; QRT-PCR, quantitative reverse transcription-polymerase chain reaction.

Quantitative Reverse Transcription-Polymerase Chain Reaction (QRT-PCR)

Total RNA was isolated from tissues, and PAM cells using Trizol reagent (15596026, Thermo Fisher Scientific, Waltham, MA, USA). RNA concentration was quantified on a spectrophotometer (NanoDrop ND-1000, Thermo Fisher Scientific, Waltham, MA, USA). Subsequently, 1 µg of total RNA was reverse-transcribed into cDNA using a cDNA synthesis kit (DRR037A, Takara, Dalian, China). Quantitative real-time PCR was carried out on a LightCycler 96 system (Roche Diagnostics, Basel, Switzerland) with Eastep qPCR Master Mix (LS2062, Promega, Madison, WI, USA). The amplification protocol consisted of an initial step at 95 °C for 10 min, followed by 40 cycles of 95 °C for 30 s and 60 °C for 30 s. *GAPDH* expression was used as an internal control for data normalization, and relative gene expression levels were calculated via the $2^{-\Delta\Delta Ct}$ method [22]. Sequences of the gene-specific primers are provided in Table 1.

Immunoprecipitation (IP) and Ubiquitination Analyses

SiBTRC and pCMV-HA-Ub (HG-VFH1037, Honorgene, Changsha, China) were co-transfected into PAM for incubation (48 h). With IP kit (abs955, Absin, Shanghai, China), the cells were treated with 20 µM MG-132 (S1748-25mg, Beyotime, Shanghai, China) (4 h), and cell lysates were prepared using lysis buffer. 500 µL cell lysate was incubated with 5 µg anti-ULK1 (1:1000, ab229909, Abcam, Cambridge, UK) or control IgG (1:100, ab172730, Abcam, Cambridge, UK) (1 h, 4 °C). Next, cell lysates were reacted with 5 µL Protein A and 5 µL Protein G (3 h) and centrifuged (1 min, 12,000 ×g). Afterwards, SDS-PAGE sample loading buffer (P0015, Beyotime, Shanghai, China) was added into cell lysate and centrifuged. Western blot was carried out with anti-HA tag antibody (ab236632, Abcam, Cambridge, UK) to detect ULK1 ubiquitination.

Data Analyses

All data from three independent assays were depicted by mean ± standard deviation (SD) and analyzed in GraphPad Prism 8 (GraphPad, Inc., La Jolla, CA, USA). One-way Analysis of Variance (ANOVA) was used for multi-group comparisons followed by Tukey's post-hoc test. The statistical significance was defined when p-value < 0.05.

Results

PAK Infection Caused a Decrease of Bacterial Clearance in Post-TBI Pneumonia Animal Models, Which Was Reversed by siBTRC

After the mice transfected with/without siBTRC received craniotomy and PAK injection and sacrificed, examination regarding bacterial clearance in the lung tissues was completed by CFU count assay. Fig. 1A shows that the number of CFU was higher in Mod group than Sham group, hinting aggravated bacterial infection after TBI ($p < 0.001$). Importantly, transfection of siBTRC decreased the number of CFU in the lung tissues after TBI (Fig. 1A, $p < 0.001$), confirming that siBTRC increased the bacterial clearance in the lung tissues. Further, QRT-PCR result showed that the *BTRC* expression was increased in the Mod group (Fig. 1B, $p < 0.001$). However, *BTRC* expression was decreased after transfected with siBTRC, indicating the transfection was successful (Fig. 1B, $p < 0.01$).

PAK Infection Aggravated Inflammatory Infiltration and Lung Infection in Post-TBI Pneumonia Animal Models, Which Were Offset by siBTRC

Meanwhile, based on the results of ELISA assay, more inflammatory factors TNF-α, IL-6, IL-1β, and IFN-γ in BAL fluid were increased in the Mod group compared with Sham group (Fig. 1C–F, $p < 0.001$), while TNF-α, IL-6, IL-1β, and IFN-γ were less in Mod+siBTRC group than Mod+siNC group (Fig. 1C–F, $p < 0.001$). Besides, Fig. 1G shows that the lung infection was significantly aggravated in Mod group relative to Sham group. Besides, in comparison to Mod+siNC group, Mod+siBTRC group displayed significantly relieved lung infection (Fig. 1G).

PAK Infection Increased BTRC Expression, Decreased ULK1 Expression, and Inhibited Autophagy, Which Were Attenuated by siBTRC

Furthermore, western blot data showed that BTRC and P62 expressions were noticeably up-regulated in the lung tissues, whereas ULK1 expression and LC3 II/LC3 I ratio were clearly reduced (Fig. 1H–J, $p < 0.01$) in Mod Group compared to Sham group. Besides, BTRC and P62 expressions were markedly down-regulated, yet ULK1 expression and LC3 II/LC3 I ratio were elevated (Fig. 1H–J, $p < 0.01$) in Mod+siBTRC group in contrast with Mod+siNC group.

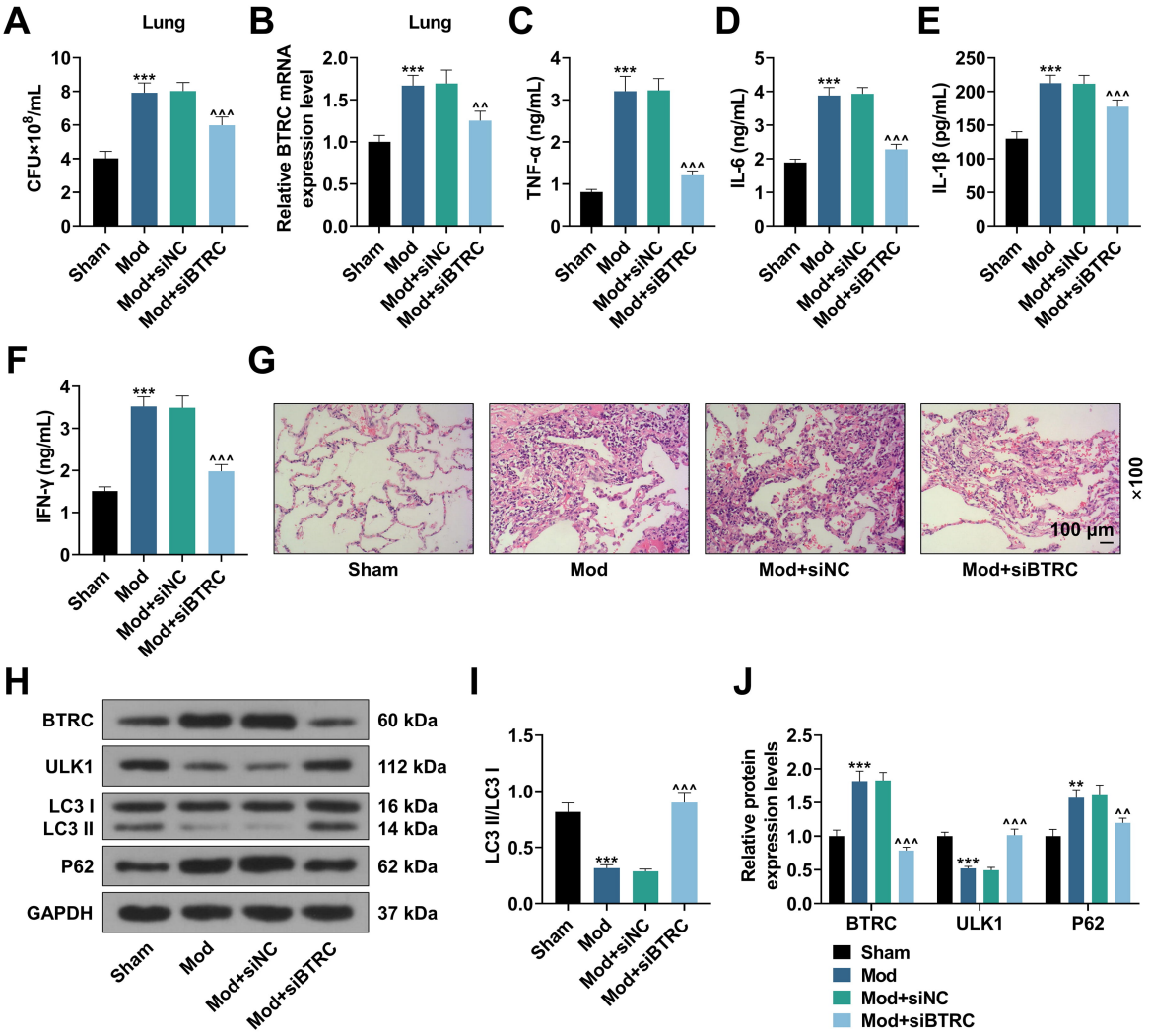

Fig. 1. The effects of siBTRC on bacterial clearance, inflammation, pathological changes, BTRC and ULK1 expressions, and autophagy in post-TBI pneumonia animal models. (A) In C57BL/6 mice undergoing craniotomy and PAK injection (25 μL) with/without siBTRC transfection and being sacrificed, the bacterial clearance in the lung tissues (CFU count assay). (B) QRT-PCR was used to measure the expression of *BTRC*. (C–F) Inflammatory factors TNF-α, IL-6, IL-1β, and IFN-γ in BAL fluid (ELISA assay). (G) In post-TBI pneumonia models, pathological changes of lung tissues (scale bar = 100 μm; magnification: ×100) (HE staining), (H–J) and BTRC, ULK1, LC3 I, LC3 II, and P62 expressions in lung tissues (western blot). GAPDH functioned as a loading control. $^{**}p < 0.01$, $^{***}p < 0.001$ vs. Sham; $^{\wedge\wedge}p < 0.01$, $^{\wedge\wedge\wedge}p < 0.001$ vs. Mod+siNC. n = 3 (mean ± SD), One-way Analysis of Variance (ANOVA) was used for multi-group comparisons. siBTRC, small interfering RNA targeting BTRC; BTRC, beta-transducin repeat containing E3 ubiquitin protein ligase; post-TBI, post-traumatic brain injury; PAK, *Pseudomonas aeruginosa* K-strain; CFU, colony forming unit; QRT-PCR, quantitative reverse transcription-polymerase chain reaction; TNF-α, tumour necrosis factor α; IL-6, interleukin 6; IL-1β, interleukin 1β; IFN-γ, interferon-γ; BAL, bronchoalveolar lavage; ELISA, enzyme-linked immunosorbent assay; HE, hematoxylin and eosin; LC3 I, microtubule-associated protein 1 light chain3 I; LC3 II, microtubule-associated protein 1 light chain3 II; P62, heat shock 90-like protein; ULK1, Unc-51 like autophagy activating kinase 1; GAPDH, glyceraldehyde-3-phosphate dehydrogenase; SD, standard deviation.

PAK Infection Suppressed Viability, Autophagy, Bacterial Killing and Phagocytosis of PAM, Which Were all Reversed by siBTRC

The purity of PAM was verified by crystal violet staining (Fig. 2A). Further, PAM are identified as a cell population that is positive for CD11c+SiglecF+CD64+ (Fig. 2B). After obtainment of PAM transfected with/without siBTRC and viability examination by CCK-8, the viability was observed to be suppressed after PAM were infected by PAK (Fig. 2C, $p < 0.001$). Importantly, PAK infection resulted in obviously promoted viability of siBTRC-transfected PAM compared with siNC-transfected cells (Fig. 2C, $p < 0.01$). Then the CFU count assay was employed to measure the bacterial killing and phagocytosis of PAM on PAK. As

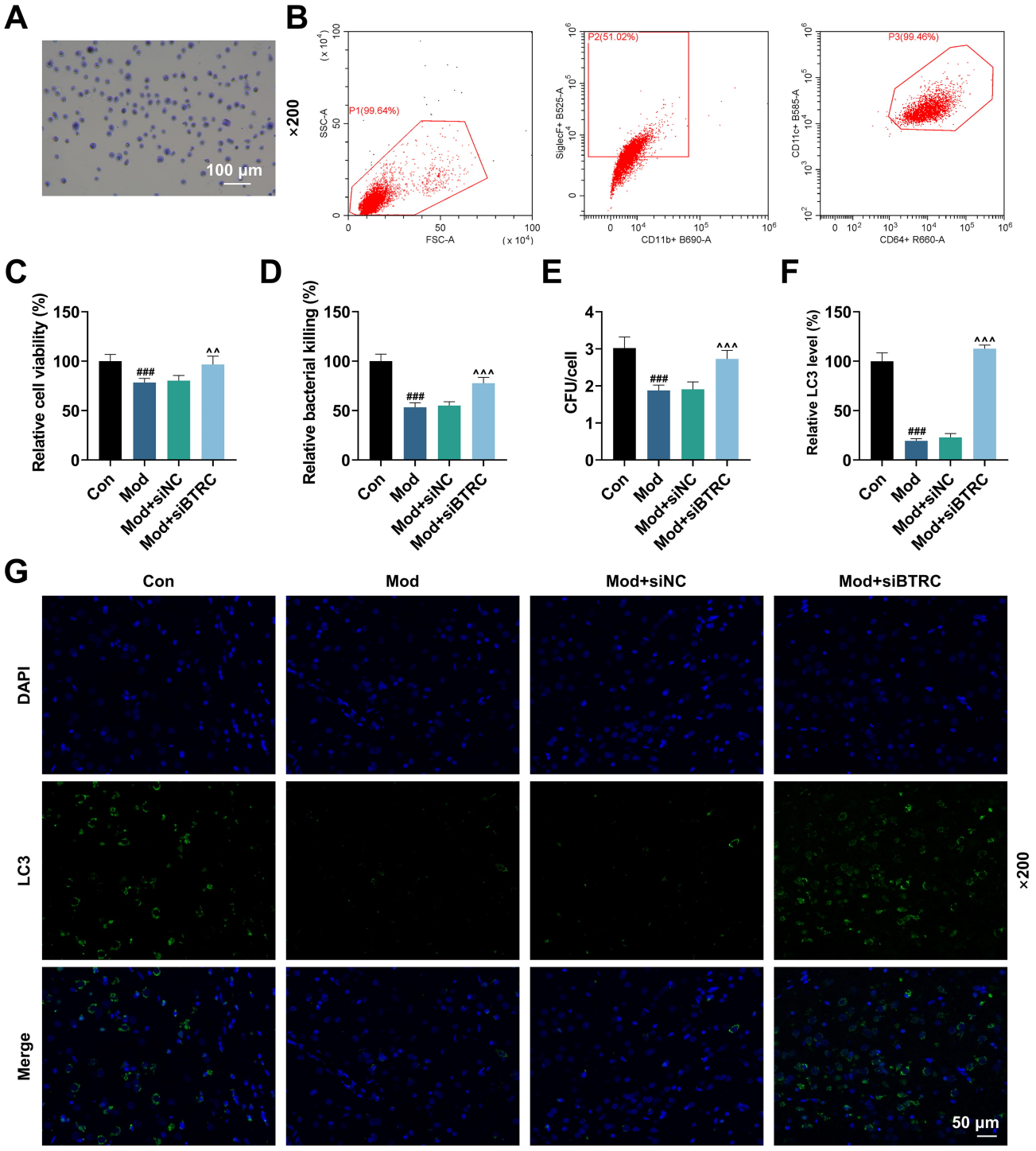

Fig. 2. The effects of siBTRC on viability, bacterial killing and phagocytosis of PAM, and LC3 expression in PAK-infected PAM. (A,B) Crystal violet staining (A) and flow cytometry (B) was used to identify PAM. (C) The obtained PAM were transfected by siBTRC and infected by the PAK in a MOI of 20:1 PAK/PAM ratio for 2 h, the viability of PAM was tested by CCK-8 assay. (D,E) Then, the intracellular killing and phagocytosis of PAM on PAK were evaluated through CFU count assay. (F,G) After transfection and PAK infection, LC3 expression was assessed by immunofluorescence staining (scale bar = 50 μm; magnification: ×200). Each experiment was independently repeated three times. $^{\#\#\#}p < 0.001$ vs. Con; $^{\wedge\wedge}p < 0.01$, $^{\wedge\wedge\wedge}p < 0.001$ vs. Mod+siNC. One-way Analysis of Variance (ANOVA) was used for comparisons among multiple groups. PAM, primary alveolar macrophages; CCK-8, cell counting kit 8; MOI, multiplicity of infection; LC3, microtubule-associated protein 1 light chain3; DAPI, 4',6-diamidino-2-phenylindole.

displayed in Fig. 2D,E, after the PAK infection, the bacterial killing and phagocytosis of PAM were inhibited ($p < 0.001$), but those of siBTRC-transfected PAM were significantly promoted relative to siNC-transfected cells (Fig. 2D,E, $p < 0.001$). Then, we measured LC3 expression in PAM transfected with/without siBTRC to further confirm the effect of siBTRC on autophagy. Fig. 2F,G shows that the ratio of green fluorescence was visibly decreased after PAK infection ($p < 0.001$). More importantly, after PAK infection, in contrast to the ratio in siNC-containing PAM, the ratio of green fluorescence was visibly elevated in the siBTRC-interfering PAM ($p < 0.001$).

PAK Infection Up-Regulated BTRC Expression, Down-Regulated ULK1 Expression, and Suppressed Autophagy in PAM, Which Were Reversed by siBTRC

As shown in Fig. 3A–E, we observed that the BTRC and P62 expressions were increased, yet the ULK1 expression and the ratio of LC3 II/LC3 I were decreased after the infection of PAK ($p < 0.001$). Interestingly, after the infection of PAK, compared with those in the PAM transfected with siNC, the BTRC and P62 expressions were decreased, yet the ULK1 expression and the ratio of LC3 II/LC3 I were increased in the PAM transfected with siBTRC (Fig. 3A–E, $p < 0.001$). Furthermore, the ULK1 ubiquitination was assessed by IP and western blot. The results of western blot reflected that PAK infection decreased the ULK1 expression, while the siBTRC increased the ULK1 expression in PAK-infected PAM before the IP assay (Fig. 3F). More importantly, the results of IP assay and western blot showed that after PAK infection, ULK1 expression in PAM treated with anti-HA tag antibody was increased (Fig. 3F). Under PAK infection, co-immunoprecipitation using anti-ULK1 antibody followed by immunoblotting with anti-HA antibody revealed a marked decrease in HA signal in siBTRC-transfected PAMs compared to the siNC group (Fig. 3F), which confirmed that siBTRC increases ULK1 expression by suppressing ubiquitination.

BTRC Regulated Macrophage Dysfunction and Inflammatory Response After PAK Infection via ULK1

QRT-PCR result showed that the expression of *BTRC* and *ULK1* was decreased after transfected with siBTRC or siULK1, indicating the transfection was successful (Fig. 4D,E, $p < 0.001$). Following PAK infection, cell viability, bacterial killing, and phagocytic capacity were reduced, accompanied by up-regulated BTRC and p62, down-regulated ULK1 and reduced LC3 II/LC3 I ratio (Fig. 4A–C,F–J, $p < 0.01$). BTRC deficiency reversed PAK-induced alterations in these parameters, while ULK1 silencing offset the effects of BTRC knockdown (Fig. 4A–C,F–J, $p < 0.01$). *In vivo* experiments demonstrated compared with the Sham group, the Mod+siNC+siNC group presented significantly elevated CFU counts and up-regulated TNF-α, IL-6, IL-1β, and IFN-γ (Fig. 5A–E, $p < 0.001$). BTRC knockdown reduced CFU counts and the secretion of these proinflammatory cytokines, which were reversed by ULK1 silencing (Fig. 5A–E, $p < 0.05$). Moreover, more severe pulmonary infection and greater inflammatory cell infiltration occurred post TBI (Fig. 5F). BTRC silencing attenuated lung inflammation, while concurrent knockdown of ULK1 reversed the anti-inflammatory effect of BTRC silencing (Fig. 5F). Western blot analysis outcomes further revealed that Mod+siNC+siNC group showed up-regulation of BTRC and p62 in lung tissues, along with decreased ULK1 and LC3 II/LC3 I ratio (Fig. 5G–I, $p < 0.001$). These changes were reversed by BTRC knockdown, while ULK1 silencing negated the regulatory effects of BTRC suppression (Fig. 5G–I, $p < 0.001$).

Discussion

Existing researches have confirmed the bacterial pneumonia as a significant factor for the poor prognosis after TBI [2,5]. Specifically, the patients with severe TBI are prone to nosocomial infections that has been increasingly considered as the main contributors to poor outcomes of TBI, especially the hospital-acquired pneumonia [5,23]. *Pseudomonas aeruginosa* is a kind of bacterial pathogen that can significantly cause the lung infection after TBI [1,6]. Accordingly, the current study used the model of post-TBI pneumonia infected by a kind of *Pseudomonas aeruginosa*, and revealed a novel way to ameliorate post-TBI lung infection. Consistently [1], we unveiled one of mechanism by which the bacterial pneumonia after TBI may be relieved is the decline of bacterial clearance. More importantly, we additionally explored the underlying mechanism of BTRC silencing on the bacterial clearance after TBI.

Prior studies have elucidated that the shortened half-life of BTRC protein leads to the accumulation of DEPTOR, which subsequently inhibits mTORC1 activation and activates autophagy [24]. Also, it is worth noting that the formation of the autophagosomes contributes to the bacterial clearance [7]. BTRC silencing can reverse the effects of LPS on LPCAT1 level in LPS-induced lung injury [25]. However, there is no report examining how BTRC silencing impacts post-TBI lung infection, enabling us to commence this research to further clarify the corresponding effects and mechanisms. In light of existing evidence, after TBI, another activated pathway is the inflammatory response at the injury site, which causes the death of nerve cells and further impairs nerve function [26–28]. Various inflammatory mediators are released after TBI, which increases inflammatory cell infiltration and induces a series of inflammatory responses, thereby aggravating the secondary cerebral edema and brain damage [28–30]. Among them, TNF-α has been recognized as a pivotal inflammatory mediator in inflammatory response, by virtue of its abilities to activate

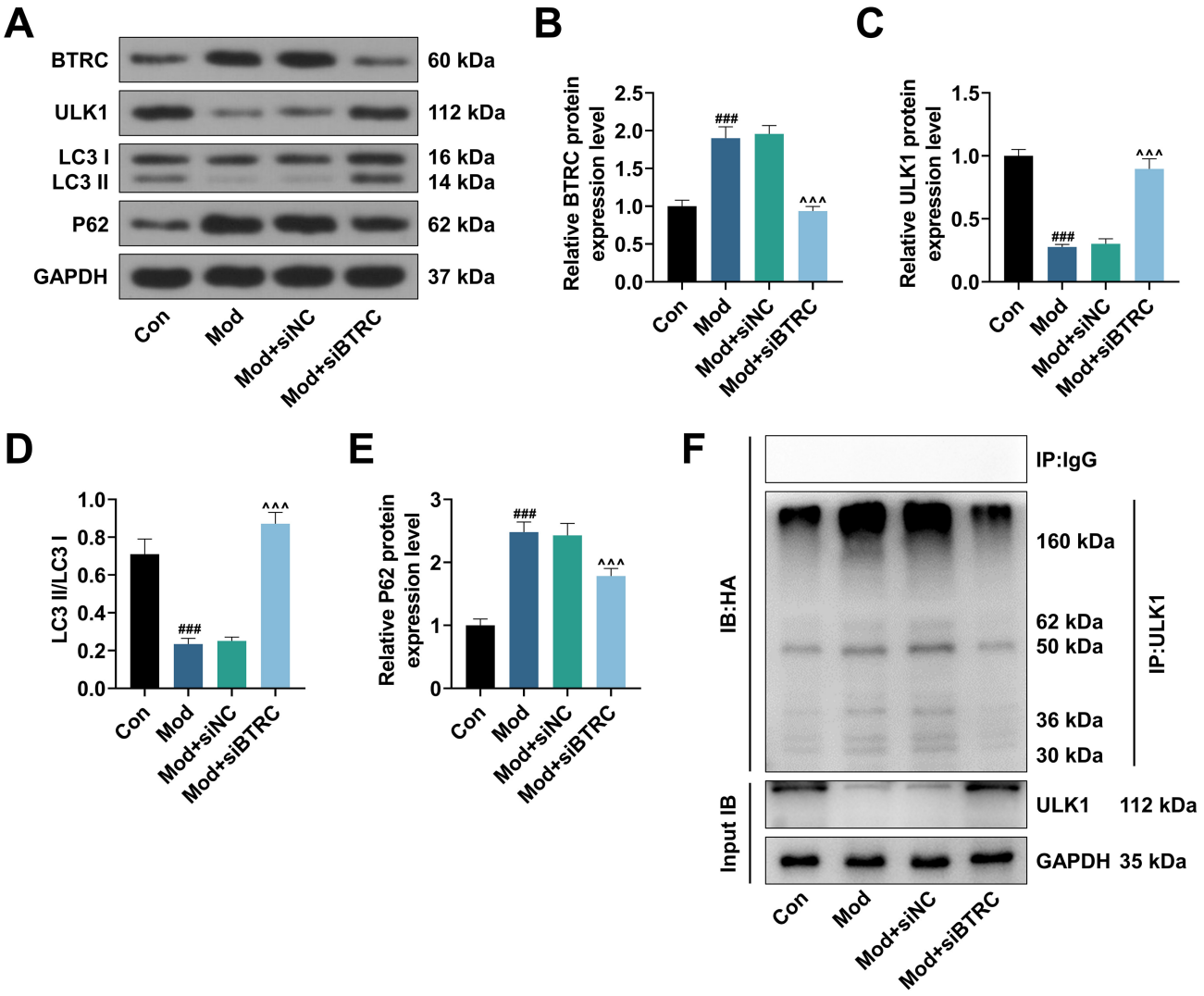

Fig. 3. The effects of siBTRC on expressions of BTRC and ULK1, autophagy, and ULK1 ubiquitination in PAK-infected PAM. (A–E) After PAM were transfected by siBTRC and infected by the PAK in a MOI of 20:1 bacteria-cell ratio ratio for 2 h, expressions of BTRC, ULK1, LC3 I, LC3 II, and P62 were tested (western blot, GAPDH as a loading control). (F) ULK1 ubiquitination in PAM (IP and western blot). Each experiment was independently repeated thrice. $^{\#\#\#}p < 0.001$ vs. Con; $^{\wedge\wedge\wedge}p < 0.001$ vs. Mod+siNC. One-way Analysis of Variance (ANOVA) was used for multi-group comparisons. IP, immunoprecipitation; IB, immunoblot; HA, hemagglutinin tag.

neutrophils and lymphocytes, and increase the permeability of vascular endothelial cells [31]. IL-1β is mainly secreted by monocytes and macrophages, participating in the body's inflammatory response [32]. IL-6 and IFN-γ are also the key stimulators of inflammatory response [33,34]. Based on the existing findings, this study further confirmed that BTRC silencing enhanced the bacterial clearance after TBI, along with the relieved inflammatory infiltration. The expression level or activity of BTRC may serve as a potential biomarker for evaluating the risk of secondary severe pulmonary infection or prognosis in TBI patients, which need further clinical verification.

Furthermore, the formation of autophagosomes contributes to bacterial clearance [7], and ULK1 is implicated in the process of autophagy and plays an active role in autophagosome formation [14,35]. ULK1 ubiquitination mediated by autophagy-related proteins and E3 ubiquitin protein ligases also participates in the autophagy [36]. In other words, the ubiquitination of ULK1 can negatively mediate ULK expression in cells to inhibit autophagy [36–38]. Notably, BTRC can grade ULK1 through ubiquitination [13]. Hence, we inferred that the effects of BTRC silencing on bacterial clearance after TBI are exerted via regulating the ULK1 ubiquitination and autophagy. As previously mentioned, LC3 is an autophagy marker [39]. When autophagy is activated, LC3 I changes to LC3 II, and the increased content of LC3 II is commonly regarded as biochemical evidence of autophagy occurrence [40]. LC3 expression is also

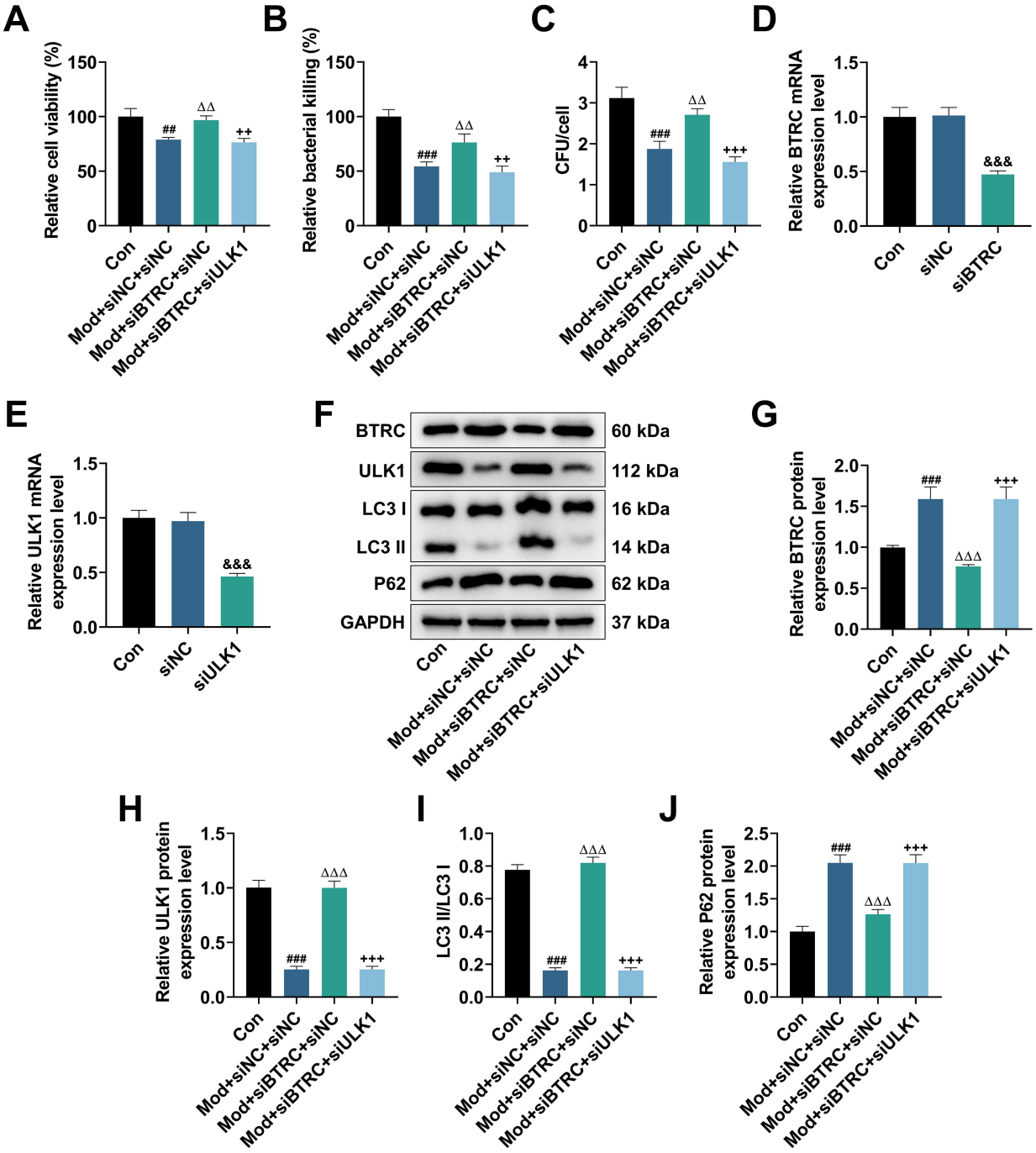

Fig. 4. The effects of siBTRC and siULK1 on viability, bacterial killing and phagocytosis of PAM, and LC3 expression in PAK-infected PAM. (A) The obtained PAM were transfected by siBTRC or siULK1 and infected by the PAK in a MOI of 20:1 PAK/PAM ratio for 2 h, PAM viability was tested (CCK-8 assay). (B,C) The intracellular killing and phagocytosis of PAM on PAK (CFU count assay). (D,E) The expression of *BTRC* and *ULK1* was detected after transfection and PAK infection (QRT-PCR). (F–J) BTRC, ULK1, LC3 I, LC3 II, and P62 expressions after transfection and PAK infection (western blot; GAPDH as a loading control). Each experiment was independently repeated thrice. $^{\#\#}p < 0.01$, $^{\#\#\#}p < 0.001$ vs. Con; $^{\&\&\&}p < 0.001$ vs. siNC; $^{\Delta\Delta}p < 0.01$, $^{\Delta\Delta\Delta}p < 0.001$ vs. Mod+siNC+siNC; $^{++}p < 0.01$, $^{+++}p < 0.001$ vs. Mod+siBTRC+siNC. One-way Analysis of Variance (ANOVA) was used for multi-group comparisons. siULK1, small interfering RNA targeting ULK1.

up-regulated in neurons after TBI [41,42]. Besides, P62, a kind of substrates, has been proved to be degraded during autophagy [27]. Herein, we demonstrated BTRC silencing plays an active role in autophagy, with up-regulated ULK1. Moreover, we also further confirmed BTRC silencing influenced bacterial clearance after TBI via activating autophagy

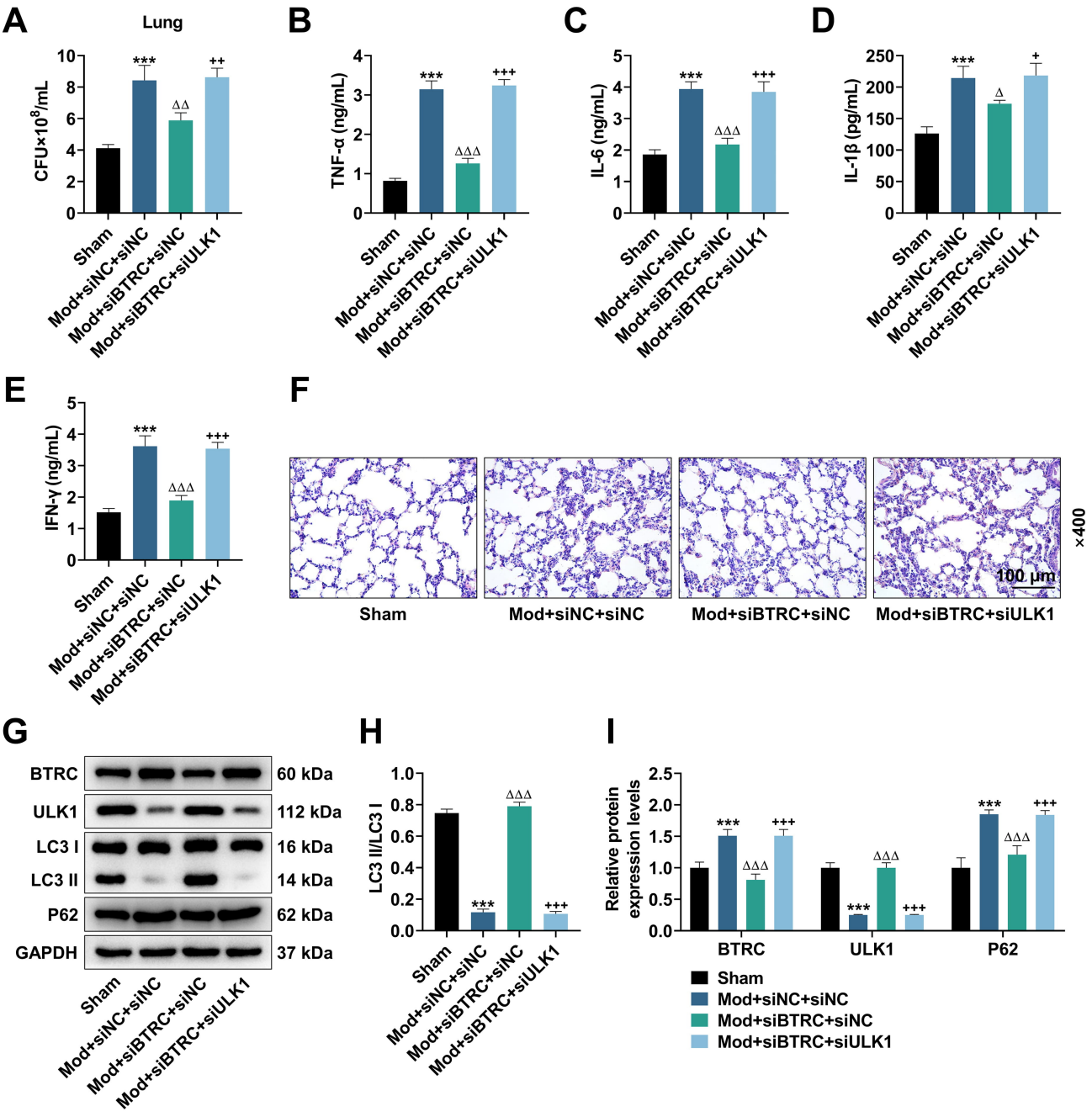

Fig. 5. The effects of siBTRC and siULK1 on bacterial clearance, inflammation, pathological changes, and autophagy in post-TBI pneumonia animal models. (A) In C57BL/6 mice undergoing craniotomy and PAK injection (25 μL) and transfected with/without siBTRC and/or siULK1, followed by sacrifice, the bacterial clearance in the lung tissues (CFU count assay). (B–E) Inflammatory factors TNF-α, IL-6, IL-1β, and IFN-γ in BAL fluid (ELISA assay). (F) In post-TBI pneumonia models, pathological changes of lung tissues (scale bar = 100 μm; magnification: ×400) (HE staining), and (G–I) BTRC, ULK1, LC3 I, LC3 II, and P62 expressionsin lung tissues (western blot, GAPDH as a loading control). Six mice per group. $^{***}p < 0.001$ vs. Sham; $^{\Delta}p < 0.05$, $^{\Delta\Delta}p < 0.01$, $^{\Delta\Delta\Delta}p < 0.001$ vs. Mod+siNC+siNC; $^{+}p < 0.05$, $^{++}p < 0.01$, $^{+++}p < 0.001$ vs. Mod+siBTRC+siNC. One-way Analysis of Variance (ANOVA) was used for multi-group comparisons.

and maintaining ULK1 stability in PAM. Importantly, further experiments demonstrated simultaneous knockdown of ULK1 reversed the role of BTRC silencing in autophagy activation, bacterial killing, and inflammatory regulation. These results underscored ULK1 as a pivotal downstream mediator in the BTRC-regulated pathway and indicated that the promoting role of BTRC knockdown in macrophage function and lung inflammation largely depended on ULK1 activity. Further, a previous study revealed that the feedback loops of adenosine monophosphate-activated protein

kinase (AMPK)-mTORC1-ULK1 regulatory triangle determine an accurate dynamical characteristic of autophagic process upon cellular stress [43]. This reminds us that AMPK-mTORC1 might also participate in the BTRC-regulated pathway, which needs additional verification. Moreover, it is necessary to develop clinically applicable BTRC inhibitors. By establishing clinically relevant infection models and combining human validation, the core role of this signaling axis (BTRC affects autophagy by regulating ULK1) in the disease should be clarified, and the entire chain of work from drug development, mechanism validation to the transformation of clinical treatment methods should be completed.

Despite the significant findings, several limitations of this study should be acknowledged. The effects of siRNA delivery alone on lung tissues should be further measured. Moreover, since this study only analyzed PAK as a pathogen, the universality of its conclusion may be limited. Subsequent research can supplement the detection of more pathogens (such as *Staphylococcus aureus*), and expand the research conclusion by comparing the test results among different infection cases. The molecular mechanisms underlying ULK1 ubiquitination regulation by BTRC require further investigation to identify specific ubiquitination sites and interacting partners. This study adopted a sample size design of n = 6 per group, which limits the ability to detect very small effects or deal with highly variable data. Future research should consider appropriately increasing the sample size if more subtle changes or highly variable indicators need to be explored. The effect of gentamicin on the viability of lung cells has not been directly detected, and the potential damage of the drug to lung tissue cannot be excluded. Furthermore, although targeting BTRC shows therapeutic potential, comprehensive *in vivo* efficacy and safety evaluations are still needed.

Conclusion

Collectively, our findings propose a novel mechanism by which BTRC silencing ameliorates bacterial pneumonia after TBI via maintaining ULK1 stability and activating autophagy to enhance bacteria-clearing capacity of macrophages. An important future direction will be to determine whether this mechanism extends to pneumonias caused by other pathogens.

Abbreviations

PAK, *Pseudomonas aeruginosa* K-strain; CFU, colony forming unit; TNF-α, tumour necrosis factor α; IL-6, interleukin 6; IL-1β, interleukin 1β; IFN-γ, interferon-γ; BAL, bronchoalveolar lavage; ELISA, enzyme-linked immunosorbent assay; BTRC, beta-transducin repeat containing E3 ubiquitin protein ligase; siBTRC, small interfering RNA targeting BTRC; ULK1, Unc-51 like autophagy activating kinase 1; LC3, microtubule-associated protein 1 light chain3; LC3 I, microtubule-associated protein 1 light chain3 I; LC3 II, microtubule-associated protein 1 light chain3 II; P62, heat shock 90-like protein; GAPDH, glyceraldehyde-3-phosphate dehydrogenase; PAM, primary alveolar macrophages; CCK-8, cell counting kit 8; MOI, multiplicity of infection; siULK1, small interfering RNA targeting ULK1; HE, hematoxylin and eosin; FBS, fetal bovine serum; SD, standard deviation; IP, immunoprecipitation; IB, immunoblot; post-TBI, post-traumatic brain injury; QRT-PCR, quantitative reverse transcription-polymerase chain reaction; DAPI, 4',6-diamidino-2-phenylindole.

Availability of Data and Materials

The datasets used and/or analyzed during the current study are available from the corresponding author upon reasonable request.

Author Contributions

LT designed the research study. LZ performed the research. LT collected and analyzed the data. LT and LZ have been involved in drafting and both authors have been involved in revising it critically for important intellectual content. Both authors have read and approved the final manuscript. Both authors have participated sufficiently in the work and agreed to be accountable for all aspects of the work.

Ethics Approval and Consent to Participate

The experimental protocol was approved by the Institutional Animal Care and Use Committee (IACUC), ZJCLA (approval number: ZJCLA-IACUC-20030109).

Acknowledgment

Not applicable.

Funding

This research received no external funding.

Conflict of Interest

The authors declare no conflict of interest.

References

[1] Pittet JF, Hu PJ, Honavar J, Brandon AP, Evans CA, Muthalaly R, *et al*. Estrogen Alleviates Sex-Dependent Differences in Lung Bacterial Clearance and Mortality Secondary to Bacterial Pneumonia after Traumatic Brain Injury. Journal of Neurotrauma. 2021; 38: 989–999. https://doi.org/10.1089/neu.2020.7327.

[2] Doran SJ, Henry RJ, Shirey KA, Barrett JP, Ritzel RM, Lai W, *et al*. Early or Late Bacterial Lung Infection Increases Mortality After Traumatic Brain Injury in Male Mice and Chroni-

cally Impairs Monocyte Innate Immune Function. Critical Care Medicine. 2020; 48: e418–e428. https://doi.org/10.1097/CCM.0000000000004273.

[3] Hui X, Haider AH, Hashmi ZG, Rushing AP, Dhiman N, Scott VK, *et al*. Increased risk of pneumonia among ventilated patients with traumatic brain injury: every day counts! The Journal of Surgical Research. 2013; 184: 438–443. https://doi.org/10.1016/j.jss.2013.05.072.

[4] Plurad DS, Kim D, Bricker S, Lemesurier L, Neville A, Bongard F, *et al*. Ventilator-associated pneumonia in severe traumatic brain injury: the clinical significance of admission chest computed tomography findings. The Journal of Surgical Research. 2013; 183: 371–376. https://doi.org/10.1016/j.jss.2013.01.036.

[5] Sharma R, Shultz SR, Robinson MJ, Belli A, Hibbs ML, O'Brien TJ, *et al*. Infections after a traumatic brain injury: The complex interplay between the immune and neurological systems. Brain, Behavior, and Immunity. 2019; 79: 63–74. https://doi.org/10.1016/j.bbi.2019.04.034.

[6] Juan C, Peña C, Oliver A. Host and Pathogen Biomarkers for Severe Pseudomonas aeruginosa Infections. The Journal of Infectious Diseases. 2017; 215: S44–S51. https://doi.org/10.1093/infdis/jiw299.

[7] Zhu P, Bu H, Tan S, Liu J, Yuan B, Dong G, *et al*. A Novel Cochlioquinone Derivative, CoB1, Regulates Autophagy in *Pseudomonas aeruginosa* Infection through the PAK1/Akt1/mTOR Signaling Pathway. Journal of Immunology. 2020; 205: 1293–1305. https://doi.org/10.4049/jimmunol.1901346.

[8] Javid A, Zlotnikov N, Pětrošová H, Tang TT, Zhang Y, Bansal AK, *et al*. Hyperglycemia Impairs Neutrophil-Mediated Bacterial Clearance in Mice Infected with the Lyme Disease Pathogen. PLoS ONE. 2016; 11: e0158019. https://doi.org/10.1371/journal.pone.0158019.

[9] Junkins RD, Shen A, Rosen K, McCormick C, Lin TJ. Autophagy enhances bacterial clearance during P. aeruginosa lung infection. PLoS ONE. 2013; 8: e72263. https://doi.org/10.1371/journal.pone.0072263.

[10] Karabiyik C, Vicinanza M, Son SM, Rubinsztein DC. Glucose starvation induces autophagy via ULK1-mediated activation of PIKfyve in an AMPK-dependent manner. Developmental Cell. 2021; 56: 1961–1975.e5. https://doi.org/10.1016/j.devcel.2021.05.010.

[11] Shaid S, Brandts CH, Serve H, Dikic I. Ubiquitination and selective autophagy. Cell Death and Differentiation. 2013; 20: 21–30. https://doi.org/10.1038/cdd.2012.72.

[12] Cui D, Dai X, Shu J, Ma Y, Wei D, Xiong X, *et al*. The cross talk of two family members of β-TrCP in the regulation of cell autophagy and growth. Cell Death and Differentiation. 2020; 27: 1119–1133. https://doi.org/10.1038/s41418-019-0402-x.

[13] Deng R, Zhang HL, Huang JH, Cai RZ, Wang Y, Chen YH, *et al*. MAPK1/3 kinase-dependent ULK1 degradation attenuates mitophagy and promotes breast cancer bone metastasis. Autophagy. 2021; 17: 3011–3029. https://doi.org/10.1080/15548627.2020.1850609.

[14] Li R, Tan S, Yu M, Jundt MC, Zhang S, Wu M. Annexin A2 Regulates Autophagy in Pseudomonas aeruginosa Infection through the Akt1-mTOR-ULK1/2 Signaling Pathway. Journal of Immunology. 2015; 195: 3901–3911. https://doi.org/10.4049/jimmunol.1500967.

[15] Liu J, Yuan Y, Xu J, Xiao K, Xu Y, Guo T, *et al*. β-TrCP Restricts Lipopolysaccharide (LPS)-Induced Activation of TRAF6-IKK Pathway Upstream of IκBα Signaling. Frontiers in Immunology. 2018; 9: 2930. https://doi.org/10.3389/fimmu.2018.02930.

[16] Shad A, Rewell SSJ, Macowan M, Gandasasmita N, Wang J, Chen K, *et al*. Modelling lung infection with Klebsiella pneumoniae after murine traumatic brain injury. Journal of Neuroinflammation. 2024; 21: 122. https://doi.org/10.1186/s12974-024-03093-9.

[17] Li Y, Chopp M, Chen J, Wang L, Gautam SC, Xu YX, *et al*. Intrastriatal transplantation of bone marrow nonhematopoietic cells improves functional recovery after stroke in adult mice. Journal of Cerebral Blood Flow & Metabolism. 2000; 20: 1311-1319. https://doi.org/10.1097/00004647-200009000-00006.

[18] Ye Z, Izadi A, Gurkoff GG, Rickerl K, Sharp FR, Ander BP, *et al*. Combined Inhibition of Fyn and c-Src Protects Hippocampal Neurons and Improves Spatial Memory via ROCK after Traumatic Brain Injury. Journal of Neurotrauma. 2022; 39: 520–529. https://doi.org/10.1089/neu.2021.0311.

[19] Idris A, Davis A, Supramaniam A, Acharya D, Kelly G, Tayyar Y, *et al*. A SARS-CoV-2 targeted siRNA-nanoparticle therapy for COVID-19. Molecular Therapy. 2021; 29: 2219–2226. https://doi.org/10.1016/j.ymthe.2021.05.004.

[20] Juan CX, Mao Y, Cao Q, Chen Y, Zhou LB, Li S, *et al*. Exosome-mediated pyroptosis of miR-93-TXNIP-NLRP3 leads to functional difference between M1 and M2 macrophages in sepsis-induced acute kidney injury. Journal of Cellular and Molecular Medicine. 2021; 25: 4786–4799. https://doi.org/10.1111/jcmm.16449.

[21] Sarkar A, Tindle C, Pranadinata RF, Reed S, Eckmann L, Stappenbeck TS, *et al*. ELMO1 Regulates Autophagy Induction and Bacterial Clearance During Enteric Infection. The Journal of Infectious Diseases. 2017; 216: 1655–1666. https://doi.org/10.1093/infdis/jix528.

[22] Livak KJ, Schmittgen TD. Analysis of relative gene expression data using real-time quantitative PCR and the 2(-Delta Delta C(T)) Method. Methods. 2001; 25: 402–408. https://doi.org/10.1006/meth.2001.1262.

[23] Andraweera N, Seemann R. Acute rehospitalisation during the first 3 months of in-patient rehabilitation for traumatic brain injury. Australian Health Review. 2016; 40: 114–117. https://doi.org/10.1071/AH15062.

[24] Xiong X, Liu X, Li H, He H, Sun Y, Zhao Y. Ribosomal protein S27-like regulates autophagy via the β-TrCP-DEPTOR-mTORC1 axis. Cell Death & Disease. 2018; 9: 1131. https://doi.org/10.1038/s41419-018-1168-7.

[25] Zou C, Butler PL, Coon TA, Smith RM, Hammen G, Zhao Y, *et al*. LPS impairs phospholipid synthesis by triggering beta-transducin repeat-containing protein (beta-TrCP)-mediated polyubiquitination and degradation of the surfactant enzyme acyl-CoA:lysophosphatidylcholine acyltransferase I (LPCAT1). The Journal of Biological Chemistry. 2011; 286: 2719–2727. https://doi.org/10.1074/jbc.M110.192377.

[26] Pearse D, Jarnagin K. Abating progressive tissue injury and preserving function after CNS trauma: The role of inflammation modulatory therapies. Current Opinion in Investigational Drugs. 2010; 11: 1207–1210.

[27] Andersson U, Yang H, Harris H. Extracellular HMGB1 as a therapeutic target in inflammatory diseases. Expert Opinion on Therapeutic Targets. 2018; 22: 263–277. https://doi.org/10.1080/14728222.2018.1439924.

[28] van Golen RF, Reiniers MJ, Marsman G, Alles LK, van Rooyen DM, Petri B, *et al*. The damage-associated molecular pattern HMGB1 is released early after clinical hepatic ischemia/reperfusion. Biochimica et Biophysica Acta. Molecular Basis of Disease. 2019; 1865: 1192–1200. https://doi.org/10.1016/j.bbadis.2019.01.014.

[29] Cheng Y, Wang D, Wang B, Li H, Xiong J, Xu S, *et al*. HMGB1 translocation and release mediate cigarette smoke-induced pulmonary inflammation in mice through a TLR4/MyD88-dependent signaling pathway. Molecular Biology of the Cell. 2017; 28: 201–209. https://doi.org/10.1091/mbc.E16-02-0126.

[30] Weber DJ, Allette YM, Wilkes DS, White FA. The HMGB1-

RAGE Inflammatory Pathway: Implications for Brain Injury-Induced Pulmonary Dysfunction. Antioxidants & Redox Signaling. 2015; 23: 1316–1328. https://doi.org/10.1089/ars.2015.6299.

[31] Zelová H, Hošek J. TNF-α signalling and inflammation: interactions between old acquaintances. Inflammation Research. 2013; 62: 641–651.

[32] Lopez-Castejon G, Brough D. Understanding the mechanism of IL-1β secretion. Cytokine & Growth Factor Reviews. 2011; 22: 189–195. https://doi.org/10.1016/j.cytogfr.2011.10.001.

[33] Tanaka T, Narazaki M, Kishimoto T. IL-6 in inflammation, immunity, and disease. Cold Spring Harbor Perspectives in Biology. 2014; 6: a016295. https://doi.org/10.1101/cshperspect.a016295.

[34] Zhang G, Liu X, Wang C, Qu L, Deng J, Wang H, *et al*. Resolution of PMA-induced skin inflammation involves interaction of IFN-γ and ALOX15. Mediators of Inflammation. 2013; 2013: 930124. https://doi.org/10.1155/2013/930124.

[35] Liu X, Wu J, Wang N, Xia L, Fan S, Lu Y, *et al*. Artesunate reverses LPS tolerance by promoting ULK1-mediated autophagy through interference with the CaMKII-IP3R-CaMKKβ pathway. International Immunopharmacology. 2020; 87: 106863. https://doi.org/10.1016/j.intimp.2020.106863.

[36] Lee DE, Yoo JE, Kim J, Kim S, Kim S, Lee H, *et al*. NEDD4L downregulates autophagy and cell growth by modulating ULK1 and a glutamine transporter. Cell Death & Disease. 2020; 11: 38. https://doi.org/10.1038/s41419-020-2242-5.

[37] Kuang E, Qi J, Ronai Z. Emerging roles of E3 ubiquitin ligases in autophagy. Trends in Biochemical Sciences. 2013; 38: 453–460. https://doi.org/10.1016/j.tibs.2013.06.008.

[38] Nazio F, Strappazzon F, Antonioli M, Bielli P, Cianfanelli V, Bordi M, *et al*. mTOR inhibits autophagy by controlling ULK1 ubiquitylation, self-association and function through AMBRA1 and TRAF6. Nature Cell Biology. 2013; 15: 406–416. https://doi.org/10.1038/ncb2708.

[39] Bao HJ, Zhang L, Han WC, Dai DK. Apelin-13 attenuates traumatic brain injury-induced damage by suppressing autophagy. Neurochemical Research. 2015; 40: 89–97. https://doi.org/10.1007/s11064-014-1469-x.

[40] Kimura S, Fujita N, Noda T, Yoshimori T. Monitoring autophagy in mammalian cultured cells through the dynamics of LC3. Methods in Enzymology. 2009; 452: 1–12. https://doi.org/10.1016/S0076-6879(08)03601-X.

[41] Cui C, Cui J, Jin F, Cui Y, Li R, Jiang X, *et al*. Induction of the Vitamin D Receptor Attenuates Autophagy Dysfunction-Mediated Cell Death Following Traumatic Brain Injury. Cellular Physiology and Biochemistry. 2017; 42: 1888–1896. https://doi.org/10.1159/000479571.

[42] Abdullah A, Zhang M, Frugier T, Bedoui S, Taylor JM, Crack PJ. STING-mediated type-I interferons contribute to the neuroinflammatory process and detrimental effects following traumatic brain injury. Journal of Neuroinflammation. 2018; 15: 323. https://doi.org/10.1186/s12974-018-1354-7.

[43] Holczer M, Hajdú B, Lőrincz T, Szarka A, Bánhegyi G, Kapuy O. Fine-tuning of AMPK-ULK1-mTORC1 regulatory triangle is crucial for autophagy oscillation. Scientific Reports. 2020; 10: 17803. https://doi.org/10.1038/s41598-020-75030-8.